

Comparisons of MWCNTs and acidified process by HNO₃ on thermal stability by DSC and TG-FTIR

Yu-Chuan Chou · Tung-Feng Hsieh ·
Yu-Chen Hsieh · Chun-Ping Lin · Chi-Min Shu

NATAS2009 Special Issue
© Akadémiai Kiadó, Budapest, Hungary 2010

Abstract Multi-walled carbon nanotubes (MWCNTs) have remarkable properties. However, their thermal stability characteristics, which may represent potential hazards during the production or utilization stage, concern unsafe or unknown properties researches. Our aim was to analyze the thermokinetic parameters of different heating rates by differential scanning calorimetry (DSC) and thermogravimetric analyzer (TG), and then to compare thermal decomposition energy parameters under various conditions by well-known kinetic equations. MWCNTs were acidified via nitric acid (HNO₃) in various concentrations from 3 to 15 N and were characterized by means of Fourier transform infrared (FTIR) spectrometry. For original and modified MWCNTs, we further identified the thermal degradation characteristics of the functional group by TG-FTIR. Finally, we established an effective and prompt

procedure for receiving information on thermal decomposition characteristics and reaction hazard of MWCNTs that could be applied as an inherently safer design during normal or upset operation.

Keywords Differential scanning calorimetry · Inherently safer design · Multi-walled carbon nanotubes · Thermal stability characteristics · Thermogravimetric analyzer · Thermokinetic parameters

List of symbols

A	Frequency factor (min^{-1})
dT/dt	Self-heating rate ($^{\circ}\text{C min}^{-1}$)
E_a	Activation energy (kJ mol^{-1})
H_0	Initial heat flow (kJ mol^{-1})
H_T	Heat flow at temperature T (kJ mol^{-1})
k_0	Reaction rate constant ($\text{s}^{-1} \text{M}^{1-n}$)
m	Mass of reactant (g)
n	Reaction order (dimensionless)
R	Universal gas constant ($\text{J mol}^{-1} \text{K}^{-1}$)
T	Temperature ($^{\circ}\text{C}$)
t	Time (min)
T_0	Initial exothermic temperature ($^{\circ}\text{C}$)
T_m	Temperature to maximum of weight loss percentage ($^{\circ}\text{C}$)
T_p	Peak temperature ($^{\circ}\text{C}$)
V	Volume of reactant (L)
	Fractional conversion (dimensionless)
β	Heating rate ($^{\circ}\text{C min}^{-1}$)
ρ	Density of reactant (g L^{-1})
ΔH	Heat of reaction (kJ mol^{-1})
ΔH_0	Total peak area of DSC curve (kJ mol^{-1})
ΔH_d	Heat of decomposition (kJ mol^{-1})
ΔH_T	Heat of decomposition via DSC trial (kJ mol^{-1})

Y.-C. Chou · C.-M. Shu (✉)

Department of Safety, Health, and Environmental Engineering,
National Yunlin University of Science and Technology
(NYUST), 123, University Rd., Sec. 3, Douliou, Yunlin 64002,
Taiwan, ROC
e-mail: shucm@yuntech.edu.tw

T.-F. Hsieh

Department of General Education Center, Chienkuo Technology
University, 1, Chieh-Shou N. Rd., Changhua 50094, Taiwan,
ROC

Y.-C. Hsieh

Graduate Institute of Environmental Engineering, National
Central University, 300, Jhongda Rd., Jhongli, Taoyuan 32001,
Taiwan, ROC

C.-P. Lin

Department of Health and Nutrition Biotechnology, College of
Health Science, Asia University, 500, Lioufeng Rd., Wufeng,
Taichung 41354, Taiwan, ROC

Introduction

Since Iijima discovered carbon nanotubes (CNTs) in 1991 [1], many interesting categories in CNTs have emerged, including single-walled carbon nanotubes (SWCNTs), multi-walled carbon nanotubes (MWCNTs), commercial carbon nanotubes (CBTs), complex MWCNTs with aluminum oxide (MWCNTs/Al₂O₃), and modified multi-walled carbon nanotubes (mMWCNTs). Today, nanotechnology is growing very rapidly and has enormous applications from medicine to food to chemicals, the adsorption of the metal ions for environmental protection [2] and much more. However, the thermally hazardous characteristics are currently seldom investigated. Here, we made evaluations for MWCNTs and mMWCNTs, especially under high temperature [3, 4].

In this study, the thermal decomposition of MWCNTs and mMWCNTs was first characterized by differential scanning calorimetry (DSC) by comparing the unexpected reactions through the thermal curves. Then, we adopted the method of isothermal model on DSC to appraise the thermal hazards while manufacturing MWCNTs and evaluated thermokinetic parameters under isothermal conditions, ranging from 440 to 640 °C [5–11]. The DSC results could be used to acquire thermokinetic parameters by thermal curves. In accordance with the Arrhenius equation, we could obtain thermokinetic parameters, such as activation energy (E_a), frequency factor (A), reaction order (n), and reaction rate constant (k). The heat of decomposition was investigated by thermogravimetric analyzer (TG) at heating rates of 2 and 10 °C min⁻¹. Moreover, we attempted to link the data with Fourier transform infrared (FTIR) spectrometry to identify the gas phase released from the MWCNTs upon heating [12]. To forestall the system from any runaway excursions or even thermal explosion under perturbed conditions, these critical thermokinetic parameters must be obtained, analyzed, and applied for safety studies.

Experimental procedures

Tests by DSC

Scanning experiments were performed on a Mettler TA8000 system coupled with a DSC821^e measuring cell that could withstand pressure up to about 100 bar. STAR^e software was used for acquiring curve traces [13]. An aluminum standard pan was used to avoid evaporation of the CNTs during scanning. We found that the data with heating rates from 0.1 to 10 °C min⁻¹ were the best in terms of accuracy and reproducibility. For accuracy, the MWCNTs samples were scanned in the temperature range

30–640 °C and at the heating rate from 0.1 to 10 °C min⁻¹ under atmospheric air. We discovered that the thermal curves of MWCNTs for 3–8 mg were most suitable. Therefore, the amounts of materials that were tested were about 3.56 mg for MWCNTs.

Kinetic analysis by the Borchardt and Daniels method

This technique assumes the reaction follows n th-order kinetics and the Arrhenius equation. The spontaneous reaction rate can be received by using single dynamic scanning with DSC and is expressed as follows:

$$\frac{d\alpha}{dt} = k(T)(1 - \alpha)^n, \quad (1)$$

where $d\alpha/dt$, $k(T)$, α , and n are the rate of reaction (s⁻¹), the rate constant at temperature T (K), the conversion of reactant (0–1) and the reaction order, respectively. From the Arrhenius equation:

$$k(T) = k_0 e^{-E_a/RT}, \quad (2)$$

where k_0 , E_a , and R are the frequency factor (s⁻¹ M¹⁻ⁿ), activation energy (kJ mol⁻¹), and universal gas constant (8.314 J mol⁻¹ K⁻¹), respectively.

On substituting the Arrhenius equation (2) into Eq. 1, we can obtain a multiple linear equation which can be expressed in logarithmic form, as indicated by Eq 3:

$$\ln \frac{d\alpha}{dt} = \ln k_0 - \frac{E_a}{RT} + n \ln(1 - \alpha) \quad (3)$$

Multiple linear regression analysis provides the desired kinetic data by using measured values ($d\alpha/dt$, α , and T) directly from the thermal curve data. Those required parameters ($d\alpha/dt$ and α) can be readily obtained by the basic assumption that a fraction reacted ($d\alpha$) corresponds to the heat flow change (dH) from DSC [6, 7].

$$\alpha = \frac{\Delta H_T}{\Delta H_0} \quad (4)$$

$$\frac{d\alpha}{dt} = \frac{\frac{dH_T}{dt}}{\Delta H_0}, \quad (5)$$

where H_T , ΔH_T , H_0 , and ΔH_0 are the heat flow at temperature T (kJ mol⁻¹), partial area of DSC curve (kJ mol⁻¹), initial heat flow (kJ mol⁻¹), and total peak area of DSC curve (kJ mol⁻¹), respectively.

Tests by TG linked with FTIR

Experiments on the heat of decomposition were performed on a PerkinElmer Paris1 system. A platinum pan was used to measure the weight loss percentage. In TG test, a precision hang-down wire made of high temperature quartz is suspended from the balance down into the furnace. At the

end of the hang-down wire is the platinum sample pan. The furnace heating rates were from 0.1 to 200 °C min⁻¹, and the heat range of quartz furnace was from 25 to 1,000 °C [14].

The FTIR was used to identify gas phase samples from TG on time by the PerkinElmer Spectrum 100 system. In this study, the frequency range of FTIR was from 450 to 4000 cm⁻¹ [15]. In TG experiments, we used oven to dry the water of the sample at 120 °C before heating from room temperature to 900 °C, and the heating rate was 4 °C min⁻¹ under ca. 21 vol.% oxygen. As planned, the ratio of oxygen and nitrogen was 1:4 to simulate atmospheric air.

Results and discussion

Analysis for surface structure

The MWCNTs and the samples after being modified via nitric acid (HNO₃) in various concentrations from 3 to 15 N were observed by field-emission scanning electron microscope (FE-SEM), as illustrated in Fig. 1. The morphology for MWCNTs and mMWCNTs was tubular like, for which the average diameter was about 20–40 nm in arrowhead.

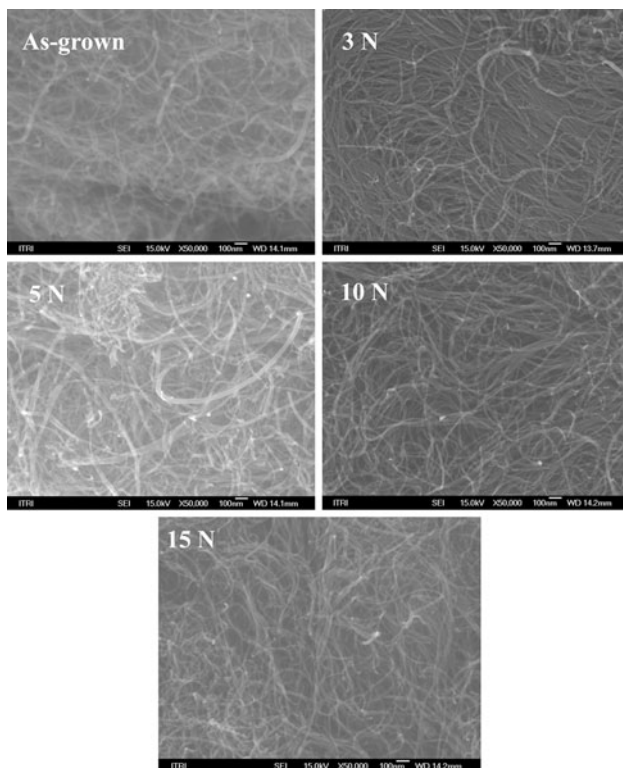


Fig. 1 Surface structure by FE-SEM tests for MWCNTs and modified via HNO₃ from 3, 5, 10, and 15 N

Dynamic thermal analyses of MWCNTs and mMWCNTs

The TG and DSC curves of MWCNTs and mMWCNTs measured at the heating rates from 0.25 to 2 °C min⁻¹ are shown in the Tables 1, 2, 3, and 4 and Figs. 2, 3, 4, and 5. The thermal decomposition for MWCNTs was analyzed by using a dynamic screening experiment and compared with mMWCNTs.

The DSC results are presented in Tables 1 and 2 and Figs. 2, 3, and 4. Here, the onset temperature (T_0) and peak temperature (T_p) for mMWCNTs conspicuously increased compared to that of MWCNTs. The T_0 of mMWCNTs was increasing when the concentration of HNO₃ was increasing. For example, for 0.25 °C min⁻¹ of heating rate, the T_0 and T_p of MWCNTs were 298 and 512 °C; whereas for the 15 N mMWCNTs, it rose to 384 and 526 °C. It indicates that the temperature of the DSC exothermic peaks for both moves substances toward the higher temperature with the increase of the concentration of HNO₃.

As a result, the oxidation of MWCNTs and mMWCNTs began about 300 °C in air and the temperature of the DSC exothermic peaks started from 512 °C and went onto exceed 606 °C. The heats of decomposition varied from about 30,360 to 38,140 J g⁻¹. Thus, the compound temperature of MWCNTs or mMWCNTs composite material during manufacturing must be lower than the oxidation temperature of the MWCNTs in air.

TG results for the MWCNTs and mMWCNTs measured at different heating rates

In Fig. 5 and Tables 3 and 4, the TG curves at the heating rates of 0.25, 0.5, 1, and 2 °C min⁻¹ are shown as the decomposition temperature for MWCNTs from 486 to 551 °C, 3 N mMWCNT from 489 to 578 °C, 5 N mMWCNT from 495 to 588 °C, 10 N mMWCNT from 505 to 595 °C, and 15 N mMWCNT from 509 to 599 °C, separately. These results reveal that the decomposition temperature of the TG moves toward a higher temperature with the increase of the heating rate and the concentration of HNO₃. In this study, the MWCNTs and mMWCNTs

Table 1 DSC experimental data of original MWCNTs at heating rates from 0.25 to 2 °C min⁻¹

$\beta/^\circ\text{C min}^{-1}$	$T_0/^\circ\text{C}$	$T_p/^\circ\text{C}$	$E_a/\text{kJ mol}^{-1}$
0.25	298	512	107.78 ± 0.82
0.50	305	542	137.40 ± 0.97
1.00	316	567	152.12 ± 0.72
2.00	337	601	152.06 ± 0.25

Table 2 DSC experimental data of 3, 5, 10, and 15 N acidified mMWCNTs at heating rates from 0.25 to 2 °C min⁻¹

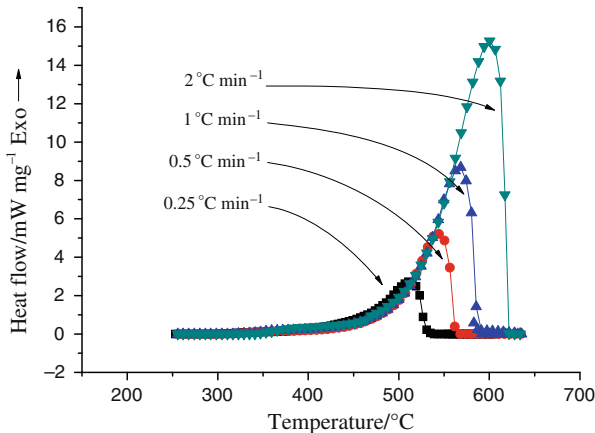
Acidified conc.	3 N			5 N			10 N			15 N		
	$\beta/^\circ\text{C min}^{-1}$	$T_0/^\circ\text{C}$	$T_p/^\circ\text{C}$	$E_a/\text{kJ mol}^{-1}$	$T_0/^\circ\text{C}$	$T_p/^\circ\text{C}$	$E_a/\text{kJ mol}^{-1}$	$T_0/^\circ\text{C}$	$T_p/^\circ\text{C}$	$E_a/\text{kJ mol}^{-1}$	$T_0/^\circ\text{C}$	$T_p/^\circ\text{C}$
0.25	284	517	119.70 ± 0.84	314	523	125.71 ± 0.08	349	526	132.92 ± 0.71	384	526	134.90 ± 0.76
0.50	340	547	152.84 ± 0.98	364	552	153.93 ± 0.57	398	555	154.99 ± 0.78	420	554	153.09 ± 0.82
1.00	358	568	152.42 ± 0.39	376	573	154.01 ± 0.59	415	578	155.03 ± 0.38	437	575	158.28 ± 0.34
2.00	376	600	150.39 ± 0.60	406	604	166.87 ± 0.40	428	606	147.31 ± 0.45	442	606	175.27 ± 0.34

Table 3 Original MWCNTs via TG tests at heating rates from 0.25 to 2 °C min⁻¹

$\beta/^\circ\text{C min}^{-1}$	$T_0/^\circ\text{C}$		$T_m/^\circ\text{C}$	
0.25		486		543
0.50		522		573
1.00		536		597
2.00		551		631

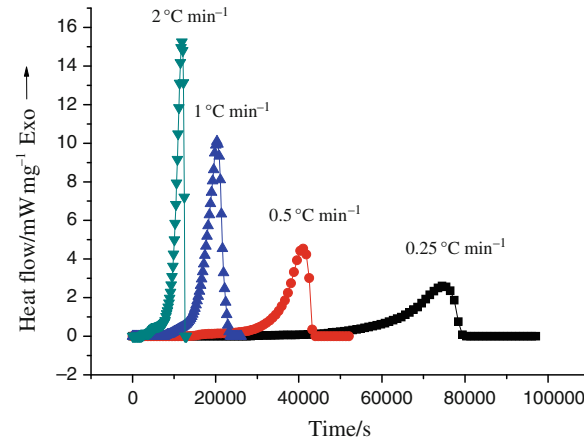
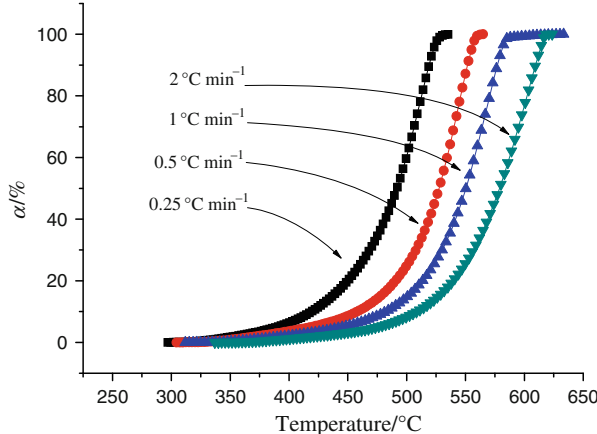
Table 4 3, 5, 10, and 15 N acidified mMWCNTs via TG tests at heating rates from 0.25 to 2 °C min⁻¹

Acidified conc.	3 N		5 N		10 N		15 N	
	$T_0/^\circ\text{C}$	$T_m/^\circ\text{C}$	$T_0/^\circ\text{C}$	$T_m/^\circ\text{C}$	$T_0/^\circ\text{C}$	$T_m/^\circ\text{C}$	$T_0/^\circ\text{C}$	$T_m/^\circ\text{C}$
0.25	489	540	495	553	505	557	509	557
0.50	526	570	540	583	544	586	547	584
1.00	563	592	565	603	567	608	569	606
2.00	578	624	588	635	595	637	599	636

**Fig. 2** DSC thermal curves of heat flow versus temperature for MWCNTs decomposition at heating rates from 0.25 to 2 °C min⁻¹

have the same phenomenon of decomposition heat as the literature [2].

The kinetic evaluation parameters were computed by our experimental data from DSC tests. Specifically, both MWCNTs and mMWCNTs thermal decomposition belong

**Fig. 3** DSC thermal curves of heat flow versus time for MWCNTs decomposition at heating rates from 0.25 to 2 °C min⁻¹**Fig. 4** DSC thermal curves of fractional conversion versus temperature for MWCNTs decomposition at heating rates from 0.25 to 2 °C min⁻¹

to zeroth order reaction in *n*th-order reaction. MWCNTs not only possess SP² bonding, but also have perfect and stable structure, high thermal conductivity and excellent electrical conductivity [16–21]. While the thermal decomposition is being stably processed, products will be accumulating in the exothermal reaction on the theory. In particular, MWCNTs have higher ΔH_d , but have lower E_a .

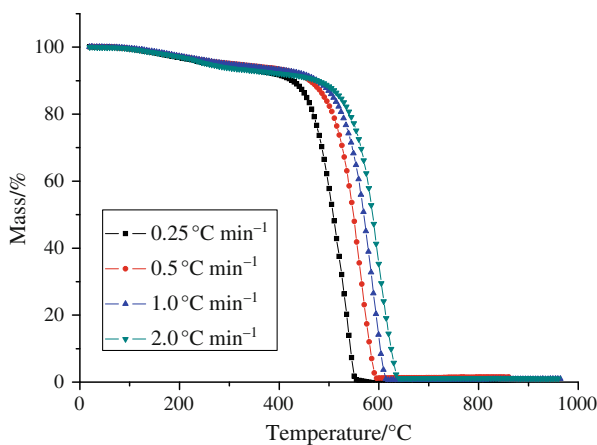


Fig. 5 TG test mass loss percentage curves of MWCNTs at heating rates from 0.25 to $2\text{ }^{\circ}\text{C min}^{-1}$

In the modification process, the carboxyl group ($-\text{COOH}$) was added to the surface of mMWCNTs that had become hydrogen bond and increased the activation energy and then the parameters moved to high temperature. As DSC and TG results, E_a , T_0 , T_p , and T_m of the modified MWCNTs increased with increasing HNO₃ concentration.

FTIR results for the MWCNTs and mMWCNTs

Figure 6 shows the FTIR spectrum of MWCNTs and 15 N mMWCNTs after TG decomposition. The CO₂ functional groups were detected at both wavenumbers of 668 and 2360 cm⁻¹. The CO₂ was from the oxidation of MWCNTs and mMWCNTs. The FTIR spectrum did not show other strong peaks and the TG results as shown in Fig. 6 indicate that the two nanomaterials have high purity in terms of quality. Since no peaks were observed beyond 3000 cm⁻¹, it seems that the functional groups are not alkenes or

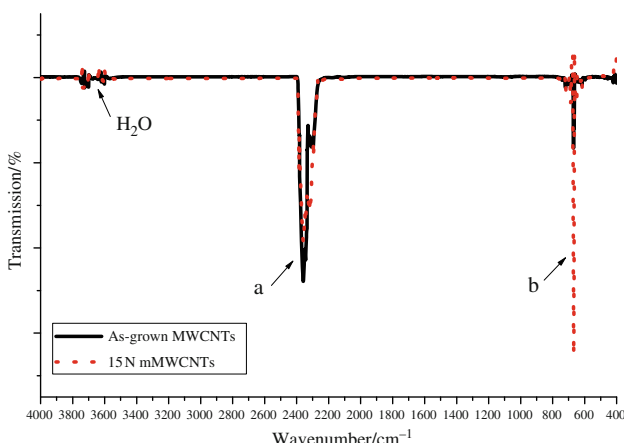


Fig. 6 Infrared spectra of MWCNTs and 15 N mMWCNTs catalyzed after TG test, the characteristic functional groups of CO₂ at **a** 2360 and **b** 668 cm⁻¹

alkynes and are not accompanied with double or triple bonds [22].

Conclusions

According to the DSC results, the MWCNTs had higher exothermic onset temperature and lower heat of decomposition than mMWCNTs. The thermal delay effect on an increasing heating rate increases the exothermic onset temperature. The TG results showed the same phenomenon in this study. The mMWCNTs added the carboxylic group on the surface which has become hydrogen bond and increases the activation energy.

In summary, for the same heating rate the mMWCNTs have less thermal hazard than MWCNTs with higher E_a and T_0 . Therefore, mMWCNTs are safer material than pure MWCNTs. The FTIR spectrum of MWCNTs and mMWCNTs after TG trials demonstrates that CNTs decomposition belongs to oxidation reaction of interest by CO₂ functional groups. Through TG results, both the MWCNTs and mMWCNTs decomposition temperatures were higher than 480 °C in air. The materials may be hazardous under high temperature and one should avoid oxygen while these are exposed to a thermal source. Moreover, the modification process by HNO₃ could make MWCNTs more stable with increase of E_a . Consequently, we substantiated that mMWCNTs' decomposition temperatures change to a higher value because of the higher E_a .

Acknowledgements The authors are indebted to the donors of the National Science Council of Taiwan under the contract no. NSC 97-2622-E-224-002-CC3 for financial support.

References

- Iijima S. Helical microtubules of graphitic carbon. *Nature*. 1991;354:56–8.
- Lu C, Chung YL, Chang KF. Adsorption of trihalomethanes from water with carbon nanotubes. *Water Res*. 2005;39:1183–9.
- Pritchard DK. Literature review—explosion hazards associated with nanopowders. USA: Crown; 2004.
- Jin J, Song M, Pan F. A DSC study of effect of carbon nanotubes on crystallization behaviour of poly (ethylene oxide). *Thermochim Acta*. 2007;456:25–31.
- Chervin S, Bodman GT. Mechanism and kinetics of decomposition from isothermal DSC data: development and application. *Process Saf Prog*. 1997;16:94–100.
- Wang YW, Shu CM, Duh YS, Kao CS. Thermal runaway hazards of cumene hydroperoxide with contaminants. *Ind Eng Chem Res*. 2001;40:1125–32.
- Shu CM, Yang YJ. Using VSP2 to separate catalytic and self-decomposition reactions for hydrogen peroxide in the presence of hydrochloric acid, temperatures and oxygen concentrations. *Thermochim Acta*. 2002;392:257–69.
- Hsieh YC, Chou YC, Lin CP, Hsieh TF, Shu CM. Thermal analysis of multi-walled carbon nanotubes by Kissinger's corrected kinetic equation. *Aerosol Air Qual Res*. 2010;10:212–8.

9. Chang CW, Chou YC, Tseng JM, Liu MY, Shu CM. Thermal hazard evaluation of carbon nanotubes with sulfuric acid by DSC. *J Therm Anal Calorim.* 2008;95(2):639–43.
10. Peng JJ, Wu SH, Hou HY, Lin CP, Shu CM. Thermal hazards evaluation of cumene hydroperoxide mixed with its derivatives. *J Therm Anal Calorim.* 2009;96:783–7.
11. Hou HY, Duh YS, Lee W, Shu CM. Hazard evaluation for redox system of cumene hydroperoxide mixed with inorganic alkaline solutions. *J Therm Anal Calorim.* 2009;95:541–5.
12. Paradise M, Goswami T. Carbon nanotubes—production and industrial applications. *Mater Des.* 2007;28:1477–89.
13. Mettler Toledo. STAR[®] Thermal Analysis. Sweden; 2005.
14. Perkin Elmer. Pyris 1 Getting Started Guide. UK; 2006.
15. Perkin Elmer. SPECTRUM 100 Series Getting Started Guide. UK; 2006.
16. MWCNTs 2040 COA. Conyuan Biochemical Technology Co. Ltd., Taipei, Taiwan, ROC. <http://www.cbt.com.tw>.
17. Berber S, Kwon YK, Tománek D. Unusually high thermal conductivity of carbon nanotubes. *Phys Rev Lett.* 2000;84(20):4613–6.
18. Kim P, Shi L, Majumdar A, McEuen PL. Thermal transport measurements of individual multiwalled nanotubes. *Phys Rev Lett.* 2001;87(21):225502-1–4.
19. Xie H, Cai A, Wang X. Thermal diffusivity and conductivity of multiwalled carbon nanotube arrays. *Phys Lett A.* 2007;369:120–3.
20. Çengel YA, Boles MA. Thermodynamics: an engineering approach. 6th ed. New York: McGraw-Hill Inc.; 2007.
21. Qi X, Boggs S. Thermal and mechanical properties of EPR and XLPE cable compounds. *IEEE Electr Insul Mag.* 2006;22(3):19–24.
22. Jung YS, Jeon DY. Surface structure and field emission property of carbon nanotubes grown by radio-frequency plasma-enhanced chemical vapor deposition. *Appl Surf Sci.* 2002;193:129–37.